Shell Model and the Levels of Zr^{91}†

S. RAMAVATARAM
Cyclotron Laboratory, Department of Physics, The University of Michigan, Ann Arbor, Michigan
(Received 11 May 1964)

A shell-model interpretation of low-lying positive-parity states of Zr^{91} has been attempted by taking into account the residual interactions between the two protons in the $2p_{1/2}$ and $1g_{9/2}$ configurations coupled to a neutron in the $2d_{5/2}$, $3s_{1/2}$, $1g_{7/2}$, and $2d_{3/2}$ single-particle states. A finite-range, central two-body force with a Gaussian radial dependence was assumed. Data on other nuclei in this mass region have been analyzed to provide a set of model parameters. Qualitative agreement has been obtained with the experimental data on Zr^{91}.

I. INTRODUCTION

THE general validity of simple shell-model configurations in the mass-90 region has been indicated by several authors.[1–3] The reasonable agreement with experiment that has been obtained by them supports the underlying assumption that 38 protons and 50 neutrons form relatively good closed shells.

The transition strengths and the l_n values in the $Zr^{90}(d,p)Zr^{91}$ reaction[4] suggest that although the ground state of Zr^{91} belongs predominantly to a $2d_{5/2}$ neutron configuration, considerable fragmentation of the $3s_{1/2}$, $1g_{7/2}$, and $2d_{3/2}$ single-particle states occurs. An attempt has been made to interpret these core excitations by coupling a neutron in the above single-particle states (νnlj_n) to the positive parity states of the Zr^{90} core

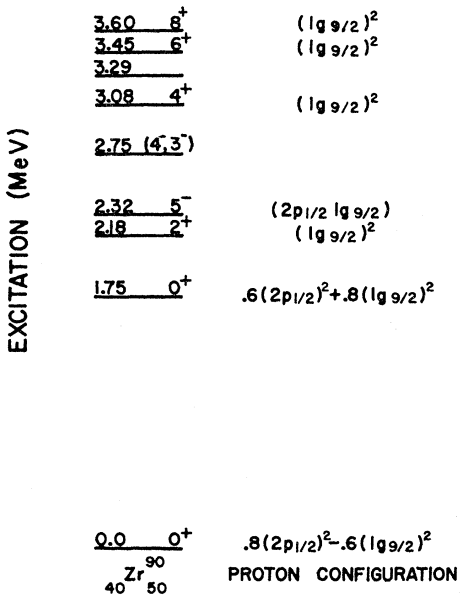

FIG. 1. Energy levels of Zr^{90} and their suggested configurations (Ref. 3).

(Fig. 1). Such an interpretation of states of Zr^{91} requires estimates of the neutron-proton interaction in the configurations $(\pi 2p_{1/2}\nu nlj_n)$ and $(\pi 1g_{9/2}\nu nlj_n)$, respectively. The importance of determining the matrix elements of the two-body effective interaction from experimental data rather than from purely phenomenological shell-model potentials has been stressed by Talmi.[1,2] However, in this mass region, while experimental estimates of the $n-p$ interaction in the relevant $(\pi 2p_{1/2}\nu nlj_n)$ configurations are available, considerably less is known regarding the $(\pi 1g_{9/2}\nu nlj_n)$ configuration; the only information obtained experimentally so far concerns the lowest configuration, viz. $(\pi 1g_{9/2}{}^2\nu 2d_{5/2})$. This situation necessitates the use of a phenomenological model (Sec. II) to compute the matrix elements of the residual interaction in the remaining $(\pi 1g_{9/2}\nu nlj_n)$ configurations. In this paper, although a phenomenological approach had to be used, the arbitrary parameters of the model calculation in Zr^{91} were obtained by analyzing the data on the $(\pi 2p_{1/2}\nu nlj_n)$ and $(\pi 1g_{9/2}{}^2\nu 2d_{5/2})$ configurations (Sec. III). The results of the calculation in Zr^{91} and comparison with experiment are dealt with in Sec. IV.

II. THEORETICAL

The nuclear Hamiltonian can be written as:

$$H=H_{\text{S.P.}}+H_{\text{int}}. \tag{1}$$

where $H_{\text{S.P.}}$ is the particle Hamiltonian. H_{int} is assumed to be a sum of two-particle interactions. In the positive parity states of Zr^{90} core (Fig. 1) the two extra-core protons are equivalent and H_{int} reduces to

$$H_{\text{int}}=V_{pp}+2V_{np}. \tag{2}$$

The shell-model wave function

$$\psi^0{}_{JM}(J_p,j_n)=|(\pi j_p)^2 J_p,\nu j_n;JM\rangle \tag{3}$$

is an angular-momentum coupled, antisymmetrized product of single-particle harmonic oscillator wave functions. The quantum numbers J_p, j_n refer to the angular momentum of core states and of the single-particle states, respectively. The matrix elements to be

† This work was supported in part by the U. S. Atomic Energy Commission.

[1] I. Talmi and I. Unna, Nucl. Phys. **19**, 225 (1960).
[2] I. Talmi, Phys. Rev. **126**, 2116 (1962).
[3] B. F. Bayman, A. S. Reiner, and R. K. Sheline, Phys. Rev. **115**, 1627 (1959).
[4] B. L. Cohen and O. V. Chubinsky, Phys. Rev. **131**, 2184 (1963).

evaluated will be of the form:

$$\langle \Psi^f{}_{JM}|H|\psi^i{}_{JM}\rangle = \langle |H_{\text{S.P.}}|\rangle \delta_{J_p J_p'} \delta_{j_n j_n'} + \langle |V_{pp}|\rangle \delta_{J_p J_p'} \delta_{j_n j_n'} + 2\sum_{Jnp} U_f U_i \langle j_n j_p |V_{np}| j_n' j_p' \rangle_{J_{np}}. \quad (4)$$

The first term is the single-particle energy ϵ_{j_n} of the neutron state j_n and may be estimated from experimental data in this mass region. The second term refers to the proton-proton interaction in the core state J_p and is obtained from the level spacings in Zr^{90} core.

The quantities U_f, U_i in the third term are transformation coefficients[5] arising out of recoupling of three angular momenta.

The matrix elements of the neutron-proton interaction are evaluated assuming a two-body force of the form:

$$V_{np} = \{[(W+B)t(\sigma)+(W-B)s(\sigma)] + [(H+M)t(\sigma)+(H-M)s(\sigma)]P_R P_\sigma\} \times V_0 \exp\left[\frac{-r^2{}_{np}}{2\sigma^2}\right]. \quad (5)$$

The projection operators $t(\sigma)$ and $s(\sigma)$ pick out the triplet and singlet parts of the two-particle wave function. P_σ and P_R are the spin and space-exchange operators. The coefficients W, B, H, and M determine the exchange character of the residual interaction. The parameter σ characterizes the range of the neutron-proton interaction while V_0 refers to the strength of the Gaussian potential. The L-S coupling scheme is a more convenient representation to use in the computation of matrix elements of V_{np}. A transformation from the j-j coupling [Eq. (3)] to the L-S scheme can be carried out using the tabulated transformation coefficients.[6] The evaluation of the angular part of the matrix elements of the residual interaction is straight forward; the radial part has been computed here using the Talmi Integral Method[7] and the Moshinsky transformation technique.[8,9] A general radial matrix element of a central potential $V(r)$ in such a procedure is given by

$$\langle n_1 l_1 n_2 l_2 |V(r)| n_1' l_1' n_2' l_2' \rangle = \sum_p \sum_{nlNL} \langle nlNL|n_1 l_1 n_2 l_2\rangle \times \langle n'lNL|n_1' l_1' n_2' l_2'\rangle B(nl,n'l,p) I_p. \quad (6)$$

The quantum numbers (nl,NL) are defined in Ref. 8. The transformation brackets $\langle nlNL|n_1 l_1 n_2 l_2\rangle$ and the coefficients $B(nl,n'l,p)$ have been defined and tabulated by Brody and Moshinsky.[9] The Talmi Integral[7] I_p for a Gaussian-shape interaction and harmonic oscillator wave functions is given by

$$I_p = V_0(\lambda^2/\lambda^2+1)^{p+3/2}. \quad (7)$$

The parameter λ is defined as

$$\lambda = (m\omega/\hbar)^{1/2}, \quad (8)$$

where σ characterizes the interaction range and $(\hbar/m\omega)^{1/2}$ is the "size parameter."[9]

The neutron-proton interaction matrix elements in the configurations $(\pi 2p_{1/2}\nu nlj_n)$ and $(\pi 1g_{9/2}\nu nlj_n)$ were evaluated on a desk computer; νnlj_n refers to the various single-particle states of the 51st neutron. The arbitrary parameters of the calculation are λ, the well depth V_0 and the coefficients W, B, H and M. A set of values for these parameters were obtained from considerations outlined in Sec. III.

The matrix diagonalization was carried out on the Michigan IBM-7090 computer to give eigenvalues and final-state wave functions

$$\psi_{JM} = \sum_{J_p, j_n} \alpha_J{}^{J_p, j_n} \psi^0{}_{JM}(J_p, j_n). \quad (9)$$

The spectroscopic factor $S(j_n)$ for a given fragment of the single-particle level j_n is

$$S(j_n) = (\alpha_{J=j_n}{}^{J_p, j_n})^2. \quad (10)$$

III. SHELL-MODEL PARAMETERS FROM EXPERIMENTAL DATA

Estimates of the neutron-proton residual interaction in the configurations $(\pi 2p_{1/2}\nu nlj_n)$ and $(\pi 1g_{9/2}\nu 2d_{5/2})$ configurations are available from the data on Y^{90} and Nb^{92}. A set of values for the parameter of the phenomenological potential V_{np} (Eq. 5) can be obtained from these estimates as discussed in the following.

Y^{90}

In a simple shell-model picture, the low-lying negative-parity doublets observed in the $Y^{89}(d,p)Y^{90}$ reaction[10] arise out of the configurations $(\pi 2p_{1/2}\nu nlj_n)$. Similarly, the two positive parity states reported[11] at about 700-keV excitation may be identified with the configuration $(\pi 1g_{9/2}\nu 2d_{5/2})$.

Assuming various exchange mixtures[12–14] the neutron-proton interaction in the $(\pi 2p_{1/2}\nu 2d_{5/2})$ configuration has been calculated following the procedure outlined in Sec. II. In Fig. 2 the predicted doublet splitting is com-

[5] M. Rotenberg, R. Bivins, N. Metropolis, and J. K. Wooten Jr., *The 3-j and 6-j Symbols* (The Technology Press, Cambridge, Massachusetts, 1959).
[6] J. M. Kennedy and M. J. Cliff, Atomic Energy of Canada, Report No. CRT-609, Chalk River, Ontario, 1955 (unpublished).
[7] I. Talmi, Helv. Phys. Acta. **25**, 185 (1952).
[8] M. Moshinsky, Nucl. Phys. **13**, 104 (1959).
[9] T. A. Brody and M. Moshinsky, *Tables of Transformation Brackets* (Monografas del Instituto de Fisica, Mexico City, 1960).
[10] A. W. Hamburger and E. W. Hamburger, Phys. Letters **4**, 223 (1963).
[11] Nuclear Data Sheets, compiled by K. Way *et al.* (Printing and Publishing Office, National Academy of Sciences—National Research Council, Washington 25, D. C.).
[12] B. H. Flowers, in *Proceedings of the Rehovoth Conference on Nuclear Structure*, edited by H. J. Lipkin. (North-Holland Publishing Company, Amsterdam, 1958), p. 18.
[13] S. Meshkov and C. W. Ufford, Phys. Rev. **101**, 734 (1956).
[14] J. M. Soper, Phil. Mag. **2**, 1219 (1957).

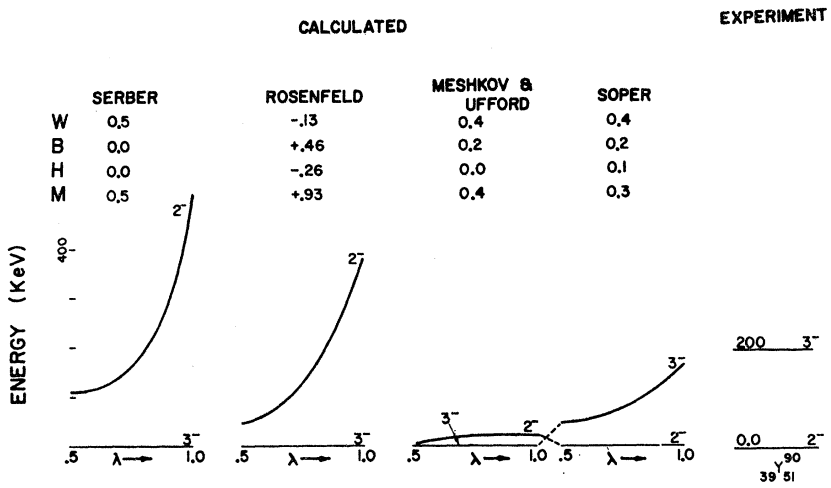

FIG. 2. Calculated $(\pi 2p_{1/2}\nu 2d_{5/2})_{2^-,3^-}$ doublet splitting for various exchange mixtures and comparison with experiment.

pared with experiment.[10] The Soper exchange mixture[14] predicts the correct spin sequence and reproduces the measured doublet separation reasonably well.

Considering the excited states of Y^{90}, we note that the nuclear Hamiltonian [Eq. (1), Sec. II] now involves the single-particle energies of the extra-core proton and neutron and H_{int} is given simply by V_{np}. Thus

$$H=(H_{\text{S.P.}})_n+(H_{\text{S.P.}})_p+V_{np}. \tag{11}$$

Rough estimates of the single-particle energies were obtained from available information in this mass region[15,16] and are summarized in Table I. The neutron-proton residual interaction V_{np} in the various excited state configurations is calculated assuming a Soper mixture and over a range of values for the parameter λ. Table II indicates the correspondence between λ and σ, the range parameter of the Gaussian interaction [Eq. (5)].

TABLE I. Estimated single particle energies of the 39th proton and 51st neutron.

Proton configuration	Energy (MeV)	Neutron configuration	Energy (MeV)
$2p_{1/2}$	0	$2d_{5/2}$	0
$1g_{9/2}$	0.730	$3s_{1/2}$	1.25
...	...	$2d_{3/2}$	2.50
...	...	$1g_{7/2}$	2.70

TABLE II. Correspondence[a] between parameter λ and σ, the range parameter of the Gaussian.

λ	$\sigma(10^{-13}$ cm)
0.5	0.96
0.75	1.44
1.0	1.92

[a] See, for example, Ref. 3.

[15] B. L. Cohen, Phys. Rev. **125**, 1358 (1962).
[16] Y. E. Kim, Phys. Rev. **131**, 1712 (1963).

The predicted level scheme is plotted as a function of λ and compared with recent experimental data[17] on Y^{90}. The best over-all agreement is obtained (Table III) using Soper exchange mixture, λ of 0.5 and $V_0=-40.0$ MeV. It may be noted that the single-particle energies required to fit the data (Fig. 3) are in reasonable agreement with the estimated values given in Table I.

Predictions of the Serber force for the same set of parameters have been included in Table III. While the Serber force cannot reproduce the observed spin sequence for the low-lying levels of Y^{90}, the agreement with experiment at higher excitations is reasonable. A comparison with results of a calculation including central plus tensor forces[16] indicates (Table III) that the experimental data may be equally well interpreted by using

TABLE III. Calculated energy levels of Y^{90} and comparison with experiment.

	Theory							
	Soper[a]		Serber[a]		Central and tensor forces[b]		Experiment[c]	
Proton-neutron configurations	J^π	Excn. (MeV)	J^π	Excn. (MeV)	J^π	Excn. (MeV)	J^π	Excn. (MeV)
$2p_{1/2}2d_{5/2}$	2^-	0.000	3^-	0.000	2^-	0.000	2^-	0.000
	3^-	0.046	2^-	0.112	3^-	0.029	3^-	0.202
$1g_{9/2}2d_{5/2}$	7^+	0.709	2^+	0.742	7^+	0.873	7^+	0.683
	2^+	0.828	7^+	0.822	2^+	0.893	2^+	0.777
$2p_{1/2}3s_{1/2}$	0^-	1.136	0^-	1.286	0^-	1.188	0^-	1.214
	1^-	1.321	1^-	1.286	1^-	1.250	1^-	1.374
$2p_{1/2}2d_{3/2}$	2^-	2.419	2^-	2.508	2^-	2.166	2^-	2.504
	1^-	2.659	1^-	2.624	1^-	2.332	1^-	2.627
$2p_{1/2}1g_{7/2}$	4^-	2.989	4^-	3.088	4^-	2.443	4^-	3.002[d]
	3^-	3.126	3^-	3.124	3^-	2.570	3^-	3.164

[a] Present calculation using $\lambda=0.5$ and $V_0=-40.0$ MeV.
[b] Ref. 16.
[c] Experimental results are from Refs. 11, 17.
[d] The excitation energies and spin assignments for the levels of the configuration $(\pi 2p_{1/2}\nu 1g_{7/2})$ are different from those given in Ref. 10. However, a reinvestigation of the $Y^{89}(d,p)Y^{90}$ reaction has confirmed the results of Robson *et al.* (Ref. 17). (C. E. Watson, private communication.)

[17] D. Robson, J. D. Fox, J. A. Becker, P. Richard, C. F. Moore, *et al.*, Technical Report, Tandem Accelerator Laboratory, Florida State University, Tallahassee, Florida, 1964 (unpublished).

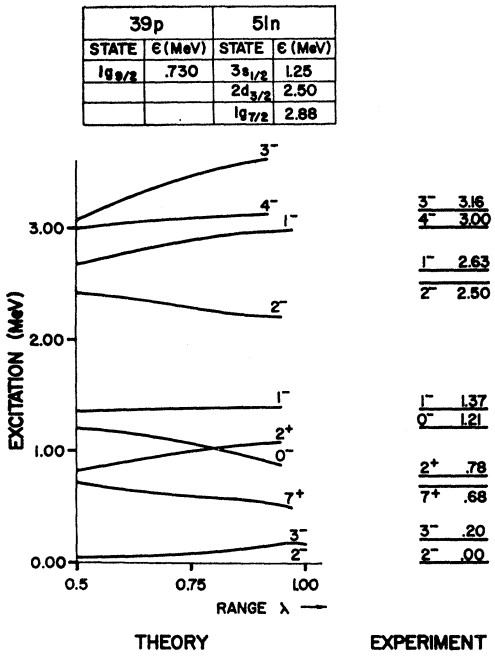

FIG. 3. Y^{90}—the predicted level sequence using Soper exchange mixture and well depth $V_0=-40.0$ MeV as a function of λ and comparison with experiment (Ref. 17). The single-particle energies used to fit data are summarized in the inset.

(as in the present work) a finite-range central force with suitable exchange character.

Nb^{92}

Low-lying positive-parity levels of Nb^{92} would arise mainly out of coupling a $2d_{5/2}$ neutron to the proton configuration $[(\pi 2p_{1/2})_0{}^2\pi 1g_{9/2}]_{9/2+}$. However, Talmi and Unna[1] have indicated that the ground state of Nb^{91} has a small admixture of the $[\pi(1g_{9/2})^3]_{9/2+}$ configuration. In the following, a neutron in the $2d_{5/2}$ and $3s_{1/2}$ single-particle states is coupled to positive-parity Nb^{91} core states (Fig. 4).

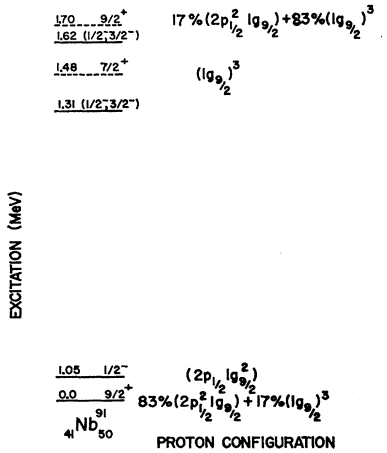

FIG. 4. Energy levels of Nb^{91} and their possible configurations (Ref. 1).

CONFIGURATION	WAVE FUNCTION	PARTICLE Nº. AND ANGULAR MOMENTUM
I. $\left[(\pi 2p_{1/2})^2\ \pi 1g_{9/2}\nu nlj_n\right]$	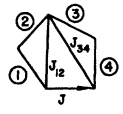	1=2=$\pi 2p_{1/2}$; 3=$\pi 1g_{9/2}$ 4=νnlj_n
II. $\left[(\pi 1g_{9/2})^3_{J_{123}}\nu nlj_n\right]$	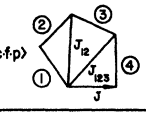	1=2=3=$\pi 1g_{9/2}$ 4=νnlj_n

FIG. 5. Configurations of the four extra-core nucleons in Nb^{92} and the corresponding wave functions in French notation (Ref. 18). Antisymmetry is ensured by restricting J_{12} to even values. The fractional parentange coefficients (c.f.p.) for the $(1g_{9/2})^3$ configuration may be obtained, for example, from de-Shalit and Talmi [*Nuclear Shell Theory* (Academic Press Inc., New York, 1963)].

Core states above 2.0 MeV and single-particle states of the neutron beyond the $3s_{1/2}$ state can be neglected in this calculation from energy considerations.

Shell-model wave functions in this four-nucleon problem are more conveniently expressed in French notation[18] (Fig. 5). The interaction Hamiltonian may be written as

$$H_{\rm int}=V_{pp}+2V_{24}+V_{34} \quad \text{or} \quad V_{pp}+3V_{34}\,, \qquad (12)$$

depending on whether configuration I or II of Fig. 5 is under consideration.

The proton-proton interaction V_{pp} is obtained from the core spectrum (Fig. 4) and the interaction in the $\frac{9}{2}+$ states is taken from Talmi and Unna.[1] The neutron-proton interaction was evaluated using a value of λ equal to 0.5 and Soper exchange mixture for various values of V_0. The best fit with experiment (Fig. 6) was obtained for a well depth of -40.0 MeV and the calculated level spacings are compared with the experimental

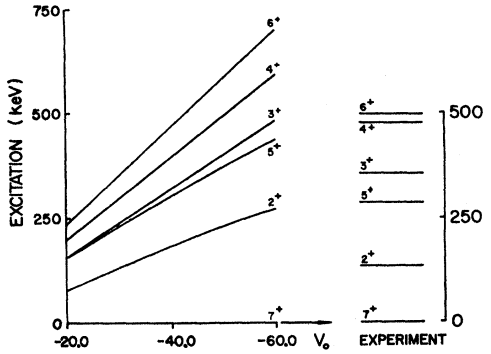

FIG. 6. Nb^{92}—variation of theoretical spectrum with well depth $V_0{}^V$ and comparison with experiment (Refs. 20, 21). Soper exchange mixture and a λ of 0.5 have been used in the calculation.

[18] M. H. MacFarlane and J. B. French, Rev. Mod. Phys. 32, 567 (1960).

TABLE IV. Calculated excitations and spin assignments for low-lying even-parity states of Nb^{92}.

Experiment[a]		Soper[b]		Serber[b]		de-Shalit[c]		Kim[d]	
J^π	Excn. (keV)	J^π	Excn. (keV)	J^π	Excn. (keV)	J^π	Excn. (keV)	J^π	Excn. (keV)
7^+	0	7^+	0	2^+	0	7^+	0	7^+	0
2^+	135	2^+	180	7^+	10	2^+	104	2^+	20
5^+	285	5^+	302	3^+	295	5^+	240	5^+	194
3^+	355	3^+	319	5^+	297	3^+	263	3^+	243
4^+	475	4^+	394	4^+	307	4^+	455	4^+	253
6^+	495	6^+	467	6^+	419	6^+	500	6^+	321

[a] Reference 19.
[b] Present calculation.
[c] Reference 20.
[d] Reference 16.

data[19,20] in Table IV. Results obtained using a Serber force ($\lambda=0.5$, $V_0=-40.0$ MeV) have also been included in Table IV and it is interesting to note that the model predictions in this case are generally in poor agreement with experiment. In particular, the Serber force predicts the 2^+ state to be lower than the 7^+ for all reasonable values of V_0. The results of calculations assuming zero-range interaction[20,21] and finite-range central plus tensor forces[16] have been included in Table IV for purposes of comparison. It is worth noting that the agreement between experimental data and the present calculations is comparable to that obtained by using more generalized interactions.

The above analysis has provided a set of values for the model parameters which may be used in phenomenological interpretation of nuclei in this mass region.

IV. Zr^{91}

Configurations involving all the positive-parity states of the core (Fig. 1) and the neutron in the single-particle states given in Table I have been considered. The proton-proton interaction was taken from the level spacings of the Zr^{90} core and from Ref. 3.

Neutron-proton interaction matrix elements were evaluated using the parameters of the two-body force obtained in Sec. III. The interaction matrices for final states of spin $\frac{5}{2}$, $\frac{1}{2}$, $\frac{7}{2}$, and $\frac{3}{2}$ were set up following the procedure outlined in Sec. II. The dimensions of the matrices ranged from 5×5 to 11×11.

Figure 7 shows a comparison of the best fit theoretical spectrum and the experimental data[4] on Zr^{91}. The first few eigenvalues and their predicted spectroscopic values for the various spin states are given in Table V.

TABLE V. Excitations and spectroscopic factors obtained from experiment and theory for Zr^{91}.

Experiment[a]			Theory		
Excn. (MeV)	l_n	S[b]	Excn. (MeV)	J^π	S
0	2	0.89	0	$5/2^+$	0.98
1.21	0	0.72	1.19	$1/2^+$	0.96
1.48	2	0.03	1.80	$5/2^+$	0.004
1.89	4	0.06	2.24	$7/2^+$	0.08
2.06	2	0.45	2.46	$3/2^+$	0.81
2.21	4	0.52	2.39	$7/2^+$	0.88
2.35	(4)	(0.05)	...	...	...
2.58	0	0.24	2.47	$1/2^+$	0.005
2.88	2	0.08	2.41	$5/2^+$	0.006
3.11	2	0.11	2.71	$3/2^+$	0.15
3.30	2	0.15	3.36	$3/2^+$	0.02
3.49[c]	4	0.33	3.45	$7/2^+$	0.01

[a] Reference 4.
[b] The spectroscopic factors for all $l=2$ transitions other than the ground state have been calculated in Ref. 4 assuming $J=\frac{3}{2}$.
[c] Experimental data suggests a group of levels at this excitation.

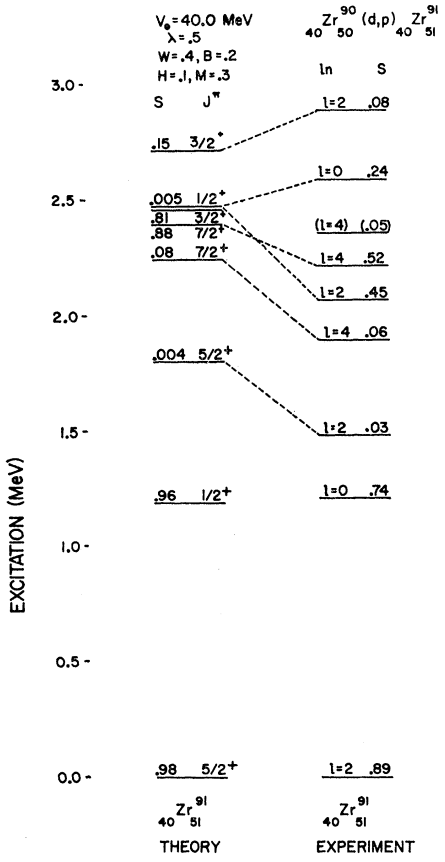

FIG. 7. Comparison between model predictions and the experimental data (Ref. 4) on Zr^{91}.

Spin-$\frac{5}{2}$ Levels

Most of the calculated $2d_{5/2}$ transition strength is predicted to be in the ground state in agreement with experiment. In addition, a weak $\frac{5}{2}$ component which may be identified with the observed 1.48-MeV level is also predicted. Experimentally, a weak $l=2$ transition is observed to this level indicating that the spin is either $\frac{3}{2}$ or $\frac{5}{2}$. The model favors a $J=\frac{5}{2}$ assignment for this level. A third weak $J=\frac{5}{2}$ level is predicted at 2.41 MeV (Table V) and may be identified with one of the weak

[19] R. F. Sweet, K. H. Bhatt, and J. B. Ball, Phys. Letters 8, 131 (1964).
[20] R. K. Sheline, C. E. Watson, and E. W. Hamburger, Phys. Letters 8, 121 (1964).
[21] A. de-Shalit, Phys. Rev. 91, 1479 (1953).

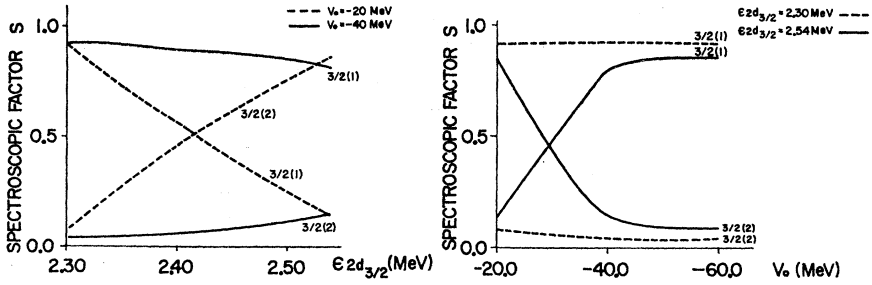

FIG. 8. Variation of the spectroscopic factor S for the first two spin $\frac{3}{2}$ levels with: (a) the $2d_{3/2}$ single-particle energy, (b) the well depth V_0.

$l=2$ transitions observed in this region of excitation (Fig. 7).

Spin-$\frac{1}{2}$ Levels

The model predicts only two spin $\frac{1}{2}$ levels below 3-MeV excitation. Although the position of the first $J=\frac{1}{2}$ level is in good agreement with experiment, the calculated strength is much larger than the observed value. Consequently, the second $J=\frac{1}{2}$ component is much weaker than the experimentally observed level at 2.58 MeV ($l_n=0$), with which it is in reasonable energy agreement. Thus, while reproducing the fragmentation in energy of the $3s_{1/2}$ single-particle state, the model accounts for the fragmentation in its strength only in a qualitative manner.

Spin-$\frac{3}{2}$ Levels

Experimentally (Fig. 7) 50% of the $2d_{3/2}$ single-particle strength is accounted for by the $l=2$ transition to the 2.06-MeV level while the remaining strength is distributed in the $l=2$ transitions observed around 3.0-MeV excitation.

In zeroth order the two lowest spin-$\frac{3}{2}$ states $(Zr^{90}{}_{2.18}+\nu 2d_{5/2})_{3/2}$ and $(Zr^{90}{}_{g.s.}+\nu 2d_{3/2})_{3/2}$ are nearly degenerate. It is clear, therefore, that the model predictions would be sensitive to small variations in the $2d_{3/2}$ single-particle energy and in the magnitude of the neutron-proton residual interaction. Figures 8(a) and 8(b) show the dependence of the calculated spectroscopic factors on these parameters. Their values for best fit ($\epsilon_{2d_{3/2}}=2.50$ MeV; $V_0=-40.0$ MeV) are, however, in good agreement with those obtained in Sec. III.

The next $J=\frac{3}{2}$ level is predicted to be weak and at 3.36-MeV excitation.

Spin-$\frac{7}{2}$ Levels

Considerations similar to those discussed in the case of spin-$\frac{3}{2}$ levels also influence the model predictions for spin-$\frac{7}{2}$ levels. The dependence of the predicted strengths of the first two spin-$\frac{7}{2}$ components on $\epsilon_{1g_{7/2}}$ and V_0 is demonstrated in Figs. 9(a) and 9(b). The best over-all agreement with experiment (Fig. 7) was obtained for a single particle energy $\epsilon_{1g_{7/2}}$ at 2.30 MeV and well depth of 40 MeV. The value of $\epsilon_{1g_{7/2}}$ is considerably lower than the estimate given in Table I (Sec. III).

The third spin-$\frac{7}{2}$ level is predicted to be above 3.0-MeV excitation suggesting that the 2.35-MeV transition (Fig. 7) may not involve the transfer of a $1g_{7/2}$ neutron.

Magnetic Moment Calculation

The observed ground-state magnetic moment[11] (−1.30 nm) is smaller than the Schmidt value (−1.91 nm) suggesting configuration admixture in the ground state of Zr^{91}. The model wave function obtained for Zr^{91} ground state is given by [Eq. (9), Sec. II] as:

$$\psi_{5/2\,5/2}=\sum_{J_p,j_n}\alpha_{5/2}{}^{J_p,j_n}\psi^0{}_{5/2\,5/2}(J_p,j_n). \qquad (13)$$

The magnetic moment for the ground state of Zr^{91} is given by:

$$\sum_{J_p'j_n',J_pj_n}\alpha_{5/2}{}^{J_p'j_n'}\alpha_{5/2}{}^{J_pj_n}\times\langle\psi^0{}_{5/2\,5/2}(J_p'j_n')\,|\,\mu\,|\,\psi^0{}_{5/2\,5/2}(J_p,j_n)\rangle. \qquad (14)$$

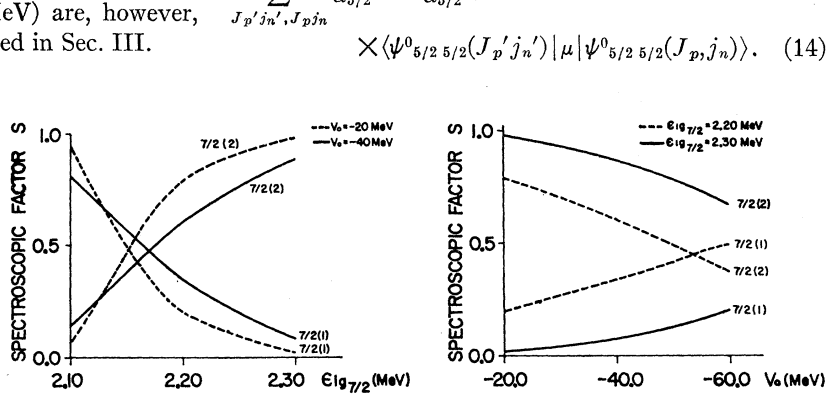

FIG. 9. Variation of the spectroscopic factor S for the first two spin-$\frac{7}{2}$ levels with: (a) single-particle energy of the $1g_{7/2}$ state, (b) well depth V_0.

TABLE VI. Comparison between free nucleon-nucleon interaction and the phenomenological two-particle interactions.

State	V_{np}	Serber	Rosenfeld	Meshkov and Ufford	Soper	Free Nucleon-Nucleon[a]
Triplet-even	$W+B+H+M$	1.00	1.00	1.00	1.00	1.00
Triplet-odd	$W+B-H-M$	0.00	−0.34	0.20	0.20	(weak)
Singlet-even	$W-B-H+M$	1.00	0.60	0.60	0.40	0.50
Singlet-odd	$W-B+H-M$	0.00	−1.80	−0.20	0.00	weak, repulsive

[a] Reference 16.

The matrix elements of Eq. (14) are evaluated following the well-known procedures for tensor operators[22] to give

$$\langle|\mu|\rangle=(-1)^{(j_n+j_n'+1)}\frac{6\sqrt{3}}{\sqrt{2}}g_s^{\nu}\delta_{ln l_n'}\delta_{Jp'}[(2j_n+1)(2j_n'+1)]^{1/2}\begin{pmatrix}1 & \frac{5}{2} & \frac{5}{2}\\ 0 & \frac{5}{2} & -\frac{5}{2}\end{pmatrix}\begin{Bmatrix} j_n' & j_n & 1\\ \frac{1}{2} & \frac{1}{2} & l_n\end{Bmatrix}\begin{Bmatrix}\frac{5}{2} & \frac{5}{2} & 1\\ j_n' & j_n & J_p\end{Bmatrix}$$

$$+(-1)^{(j_n+5/2+j_1'+j_2)}\delta_{j_n j_n'}12[(2J_p+1)(2J_p'+1)]^{1/2}\begin{pmatrix}1 & \frac{5}{2} & \frac{5}{2}\\ 0 & \frac{5}{2} & -\frac{5}{2}\end{pmatrix}\begin{Bmatrix} J_p & J_p' & 1\\ \frac{5}{2} & \frac{5}{2} & j_n\end{Bmatrix}\begin{Bmatrix} J_p' & J_p & 1\\ j_1 & j_1' & j_2\end{Bmatrix}$$

$$\times\left[g_l^{\pi}[(2j_1+1)(j_1^2+j_1)]^{1/2}+(-1)^{(l_1+s_1+j_1'+1)}\frac{\sqrt{3}}{\sqrt{2}}(g_s^{\pi}-g_l^{\pi})[(2j_1'+1)(2j_1+1)]^{1/2}\begin{Bmatrix}\frac{1}{2} & j_1' & l_1\\ j_1 & \frac{1}{2} & 1\end{Bmatrix}\right]. \quad (15)$$

The first term in Eq. (15) contains the contributions from the neutron gyromagnetic ratio g_s^{ν} and the second term involves the contributions of the two protons gyromagnetic ratios g_s^{π} and g_l^{π}. Since the model predicts 98% of the $2d_{5/2}$ strength to be in the ground-state transition, it is not surprising that the calculated magnetic moment (−1.87 nm) is only a a slight improvement on the Schmidt value (−1.91 nm).

V. CONCLUSIONS

The data on low-lying levels of three nuclei Y^{90}, Zr^{91}, and Nb^{92} have been qualitatively reproduced by a shell-model calculation involving a relatively small number of parameters. Essentially the same set of parameters of the two-body force can satisfactorily account for the observed neutron-proton interactions in the configurations $(\pi 2p_{1/2}\nu nlj_n)$ and $(\pi 1g_{9/2}\nu 2d_{5/2})$ as has been shown in Sec. III.

The agreement with experiment is less satisfactory in the case of Zr^{91} (Sec. IV). The model succeeds in qualitatively reproducing the observed fragmentation in energy and strength of the various single-particle levels (Fig. 7). The calculation indicates that the 1.48-MeV level is a $2d_{5/2}$ fragment and that the spin of the 2.35-MeV level is not $\frac{7}{2}$. The ground-state magnetic moment obtained using the model wave function is an improvement over the Schmidt value.

A variation in the $1g_{7/2}$ single-particle energy from 2.88 MeV in Y^{90} (Sec. III) to 2.30 MeV in Zr^{91} indicates an increased interaction between the two protons (which are partly in the $1g_{9/2}$ shell) of Zr^{90} and the $1g_{7/2}$ neutron. A similar effect has been observed in the variation of the $1f_{5/2}$ neutron single-particle energy in a shell-model calculation[23] on the nuclei Ti^{51}, Cr^{53}, and Fe^{55} in which there is a gradual increase in the number of $1f_{7/2}$ protons. It would be interesting to investigate, for example, via the (d,p) reaction if the $1g_{7/2}$ single-particle energy is further lowered in Nb and Mo isotopes. Such data would also provide estimates of the neutron-proton interaction in the $(\pi 1g_{9/2}\nu nlj_n)$ configurations and supplement the information discussed in Sec. III.

The correspondence between the two-body force assumed in a shell-model interpretation of residual interaction among extra-core nucleons and the free nucleon-nucleon interaction has been discussed recently.[16] It is worth noting that the Soper exchange mixture used in the present calculation has the general features of the central-force part of the free nucleon-nucleon interaction (Table VI). In Sec. III, we have seen that the inclusion of noncentral forces such as a tensor force would not necessarily result in better agreement with experiment than has been observed in the present work.

In order to improve agreement between model predictions and experiment in Zr^{91}, it may be more useful to consider inclusion of more relevant configurations rather than to think in terms of modifying the two-body force.

ACKNOWLEDGMENTS

The author is greatly indebted to Professor W. C. Parkinson for giving her the opportunity to work in the Cyclotron Laboratory; to Professor K. T. Hecht for constant advice and many helpful suggestions at every stage of the calculations. Helpful discussions with Dr. B. F. Bayman, Dr. R. D. Lawson and Dr. G. R Stachler are gratefully acknowledged.

[22] A. R. Edmonds, *Angular Momentum in Quantum Mechanics* (Princeton University Press, Princeton, 1957).

[23] J. R. Maxwell, Ph.D. thesis, The University of Michigan, 1963 (unpublished).